



**INTERNATIONAL JOURNAL OF
PHARMACEUTICAL SCIENCES**
[ISSN: 0975-4725; CODEN(USA): IJPS00]
Journal Homepage: <https://www.ijpsjournal.com>



Research Article

Engineered Nanofiber Based Carrier to Manage Arthritis and Inflammation

Dr. Omprakash Bhushure*¹, Vedant Mane², Shivam Vyavahare³, Dr. Mani Ganesh⁴,
S. G. Zingade⁵, Dr. Vijayendra Swammy⁶, Dr. Hyun Tae Jang⁷

^{1,2,3,4,5,6} Channabasweshwar College (Degree) Latur - 413512, Maharashtra, India

⁷ Department of Chemical Engineering Hanseo University, Hanseo-2gil, Haemi-myun, Seosan-si, South Korea

ARTICLE INFO

Published: 28 Jun. 2025

Keywords:

Aceclofenac, Nanofiber,
Electrospinning, Scanning
Electron Microscopy,
Fourier Transform Infrared
Spectroscopy, Differential
Scanning Calorimetry.

DOI:

10.5281/zenodo.15762721

ABSTRACT

Recent advancements in drug delivery systems have led to the exploration of loading nonsteroidal anti-inflammatory drugs (NSAIDs) onto nanodevices such as nanoparticles and nanofibers. This approach holds promise for enhancing the efficacy of arthritis treatments. In a recent review, composite nanofibers containing aceclofenac, a poorly soluble anti-inflammatory drug belonging to BCS Class-II, were developed using poly(vinyl-pyrrolidone) and co-polymer ethyl cellulose via electrospinning. The aim was to create orally disintegrating webs that could improve the solubility and dissolution rate of aceclofenac. The morphology of the resulting nanofibers was examined using scanning electron microscopy, revealing diameters in the range of a few hundred nanometers. Solid-state characterization of the samples was performed using Fourier transform infrared spectroscopy (FT-IR) and differential scanning calorimetry (DSC), indicating the amorphization of aceclofenac, which correlated with a rapid release of the active substance. By optimizing the fiber composition, particularly with 43 mg aceclofenac, 7.5% w/w PVPK90, and 10% ethyl cellulose, orally dissolving webs with fast dissolution and potential oral absorption were achieved. These findings suggest a promising avenue for enhancing the therapeutic efficacy of NSAIDs in the treatment of arthritis and related ailments.

INTRODUCTION

While nonsteroidal anti-inflammatory drugs (NSAIDs) are commonly employed in treating osteoarthritis and rheumatoid arthritis to alleviate

pain and inflammation, their mechanism of action involves inhibiting both isoforms of the cyclooxygenase enzyme (COX). However, it's primarily the inhibition of COX-2 that accounts for their analgesic and anti-inflammatory effects.

*Corresponding Author: Dr. Omprakash Bhushure

Address: Channabasweshwar College (Degree) Latur - 413512, Maharashtra, India

Email ✉: vsmane9270@gmail.com

Relevant conflicts of interest/financial disclosures: The authors declare that the research was conducted in the absence of any commercial or financial relationships that could be construed as a potential conflict of interest.



The adverse effects associated with NSAIDs, including gastrointestinal bleeding, ulcers, strokes, and heart attacks, predominantly arise from the inhibition of COX-1. The likelihood of experiencing side effects escalates with prolonged systemic exposure to NSAIDs at high doses. Aceclofenac is recognized as a potent NSAID renowned for its notable anti-inflammatory and analgesic properties. It achieves its therapeutic effects by effectively inhibiting the production of various inflammatory mediators, such as prostaglandin E2 (PGE2), tumor necrosis factors (TNF), and various interleukins (IL1- β , IL-2). Additionally, aceclofenac demonstrates chondroprotective effects through the stimulation of glycosaminoglycan synthesis. Reportedly, in double-blind studies, aceclofenac has demonstrated either greater potency or comparable anti-inflammatory effects to conventional NSAIDs. [9,10]. Aceclofenac exhibits superior gastric tolerance, attributed to its higher selectivity towards COX-2 over COX-1. This selectivity contributes to its safety profile when compared to both traditional NSAIDs and COX-2 selective inhibitors. The medication is practically insoluble in water and is categorized under the Biopharmaceutical Classification System (BCS) as Class II. Following oral administration, aceclofenac is efficiently absorbed. However, its bioavailability is compromised by significant first-pass metabolism and the drug's limited aqueous solubility. Currently, nanotechnology is a rapidly advancing field for crafting drug delivery systems characterized by dimensions typically falling within the range of 1 to 100 nanometers. Nano-carriers possess a notably high surface area to volume ratio, enabling them to mitigate the side effects commonly associated with conventional pharmaceuticals. Moreover, they excel as carriers for delivering insoluble active ingredients. Core/shell nanoscale particles were synthesized using a modified coaxial electrospinning

technique, featuring an exceptionally thin shell layer. This innovative approach facilitates the rapid dissolution of helcid, a poorly water-soluble compound. Nanofiber-based drug delivery systems leverage their expansive surface area and porosity to achieve high drug uptake. Additionally, they offer the versatility to deliver multiple drugs concurrently or serve as effective transdermal drug delivery systems. Utilizing nanofibers, orally dissolving webs can be effectively crafted, representing an innovative category of drug delivery systems with numerous advantages over traditional oral formulations, including: rapid disintegration and high dissolution rate in the oral cavity due to the large surface area, No need of water for administration; this could be an advantage in geriatrics, pediatrics, but also for dysphagic patients or patients who are unable to swallow tablets and capsules or a large amount of water, precise dosage administration in each film, Rapid absorption from the highly vascularized buccal mucosa—drugs are absorbed directly to the superior vena cava, entering into the systemic circulation without pre-systemic metabolism, Increase in bioavailability and rapid onset of action by avoiding the first-pass hepatic metabolism, while the dose can be reduced, which can lead to a reduction of side effects. The nanofibrous formulations also facilitate sustained drug release. Specifically, aceclofenac-loaded nanofibers were created using a single-nozzle electrospinning process to achieve sustained release of the drug for up to 8 hours. This approach aims to mitigate the gastrointestinal side effects associated with aceclofenac. In contrast to the combined formulation approach, our focus was on enhancing the bioavailability and reducing the gastrointestinal side effects of aceclofenac by utilizing orally dissolving nanofibrous webs. These webs offer the advantage of facilitating rapid buccal absorption of the active ingredient. The objective of the present study was to formulate



and characterize aceclofenac-loaded nanofiber-based orally dissolving webs using triethanolamine-containing polyvinylpyrrolidone (PVP) via electrospinning. The analysis encompassed morphology, thermal properties, drug content, and drug release profile of the ternary systems, aimed at determining the optimal polymer and active substance concentrations for the desired properties of potential orally dissolving webs.

EXPERIMENTAL SECTION

MATERIALS AND METHODS

Materials

The active pharmaceutical ingredient, aceclofenac (Figure 1a), was supplied by (----). Viscous polymeric solutions were prepared using poly(vinyl-pyrrolidone) (PVP K90, also known as Kollidon K90, Figure 1b), ethyl cellulose (Figure 1c), and ethanol. Phosphate buffer solution (1 M, pH 6.8) was prepared using potassium dihydrogen phosphate and disodium hydrogen phosphate for conducting the in vitro dissolution study.

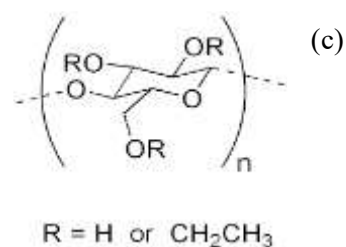
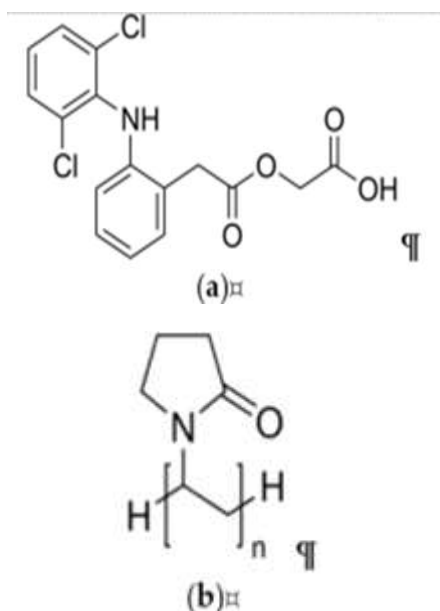


Figure No: 1. Chemical structures of (a) aceclofenac and (b) polyvinylpyrrolidone (PVP) (c) Ethyl cellulose.

Methods

Preparation of PVP Solutions Containing Aceclofenac:

Nanofibers were fabricated by adjusting the ratios of two polymers, namely Polyvinylpyrrolidone (PVP) and Ethyl cellulose. Through optimization, a specific ratio was identified, leading to the formulation V6, which exhibited favorable properties, including smoothness and convenience for drug loading.

Table.No: 2. The viscous polymeric solutions utilized in the preparation of nanofibers consisted of a blend of Polyvinylpyrrolidone (PVP K90, also known as Kollidon K90) and ethyl cellulose, along with ethanol as a solvent

Sr.No.	Sample No.	PVP Concentration	Ethyl cellulose
1	V1	1.75g	0g
2	V2	1.55g	0.2g
3	V3	1.35g	0.4g
4	V4	1.15g	0.6g
5	V5	0.95g	0.8g
6	V6	0.75g	1g
7	V7	0.6g	1.15g
8	V8	0.4g	1.35g
9	V9	0.2g	1.55g
10	V10	0.1g	1.65g

Electrospinning Process

The prepared solution was transferred into a 1 mL plastic syringe fitted with a metallic needle (22G-0.7 mm inner diameter). During the electrospinning process, the distance between the

needle and the collector was maintained at 12.5 cm, while the applied voltage was set at 18.5 kV. The flow rate for both samples and the final formulation was adjusted to 0.1 $\mu\text{L/s}$. Nanofibers were produced using the eSpin machine and collected on a grounded aluminum drum covered with aluminum foil paper.

Scanning Electron Microscopic Analysis (SEM)

The morphology of the nanofibers was examined using a scanning electron microscope (SEM). Samples were affixed to double-sided carbon adhesive tape and then coated with a sputtered gold conductive layer using the JEOL JFC-1200 Fine Coater (-----). SEM images were captured with a JEOL JSM-6380LA scanning electron microscope (-----) at magnifications of 500 \times , 1500 \times , and 5000 \times .

Fiber diameters were measured using ImageJ software (US National Institutes of Health, Bethesda, MD, USA), with measurements based on 50 randomly selected individual filaments at 5000 \times magnification. Subsequently, the average fiber diameter was calculated.

Fourier-Transform Infrared (FT-IR)

Physicochemical properties of the nanofibers were analyzed using a PekinElmer FT/IR spectrophotometer. Spectra were obtained in absorbance mode across a wavenumber range of 4000 to 400 cm^{-1} , with 100 scans conducted at a resolution of 4 cm^{-1} .

Differential Scanning Calorimetry (DSC)

Thermograms of aceclofenac, PVP, physical mixtures, and nanofibers with and without the drug were obtained using a Shimadzu DSC-60 thermal analyzer (-----). Samples were precisely weighed into aluminum pans, sealed, and subjected to scanning from 27 to 250 $^{\circ}\text{C}$ under an air

atmosphere at a rate of 10 $^{\circ}\text{C}/\text{min}$. Al_2O_3 served as the reference material.

Determination of Drug Content of Aceclofenac-Loaded Nanofibers

The absorbance of the samples was measured at the 277 nm absorption band of aceclofenac using the Shimadzu UV-1800PC UV spectrophotometer (-----). A stock solution was prepared by dissolving 100 mg of aceclofenac in 100 mL of ethanol. Then, 1 mL of this solution was further diluted to 100 mL with ethanol. From this solution, 1 mL was pipetted out and diluted with 10 mL of ethanol, resulting in a final concentration of 20 $\mu\text{g}/\text{mL}$.

Similarly, for the drug-loaded fiber, approximately 110 mg of fiber containing 20 mg of the drug was dissolved in 100 mL of ethanol. Subsequently, 1 mL of this solution was diluted to 10 mL with ethanol, resulting in a concentration of 20 $\mu\text{g}/\text{mL}$.

RESULTS AND CONCLUSION

A. Drug Characterization

1. Organoleptic properties

The drug was observed for organoleptic characteristics such as color, odor, and nature; it complies with specifications in Table

Table No. 3: Organoleptic Characteristics

Properties	Specifications	Result
Color	White to off	off
Oduor	odorless	odorless

2. Determination of melting point

The melting point of Aceclofenac was found to be 150.5 $^{\circ}\text{c}$ using a melting point apparatus in Table



Table No. 4: Determination of melting point

Parameters	Reported	Observed
Physical appearance	white crystalline powder	white crystalline powder
Melting point	149-153°C	150.5°C

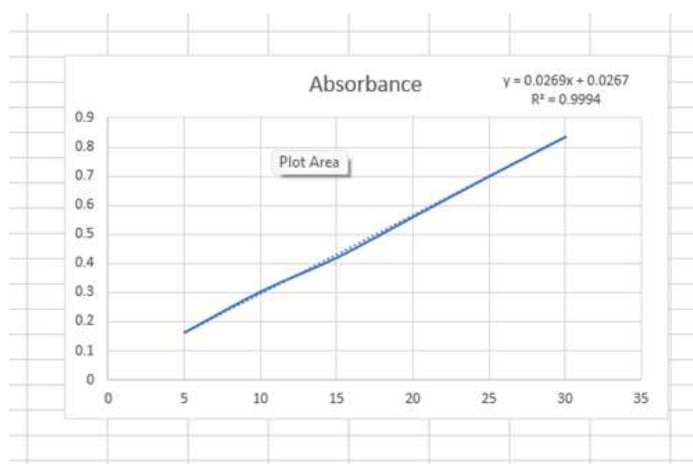
3. Solubility

The solubility of Aceclofenac is found to be as per the following Table.

Table No. 5: Solubility study

Sr. No	Solvent System	Result
1	Ethanol	Soluble
2	Water	Poorly soluble
3	Aceclofenac	Soluble
4	DMF	Soluble

4. Identification of the drug by UV spectroscopy

**Figure No.2 : Calibration curve of Aceclofenac in Electrospinning solution****Table No. 6: Calibration curve data of Aceclofenac in Ethanol & DMF**

Concentration	Absorbance
5	0.211
10	0.313
15	0.455
20	0.582
25	0.711
30	0.836

B. Identification of drug by FTIR:

The UV spectrum of Aceclofenac in electrospinning solution in the range of 200-400nm. The spectrum indicates that the observed lambda max of Aceclofenac was 277 nm which is match with lambda max given in Indian pharmacopeia.

5. Standard calibration curve of Aceclofenac

Aceclofenac shows maximum absorption at wavelength 277 nm in a electrospinning solution, standard curve was plotted by taking absorption of diluted stock solutions (5, 10, 15, 20 and 25 µg/ml)at wavelength 277 nm. The calibration curve of Aceclofenac is given below. Figure No.9

Figure 4 illustrates the FT-IR spectra of both the individual components and the nanofibers loaded with aceclofenac. In Figure 4A, the IR spectrum of pure aceclofenac displays prominent peaks, notably around 3318 cm⁻¹, likely attributed to secondary amine N-H stretching or carboxylic acid band (O-H stretching). Additionally, two ketone bands appear at approximately 1714 and 1770 cm⁻¹, along with several phenyl ring bands in the fingerprint region (Figure 4B). In Figure 4B, representing the aceclofenac-loaded sample, peaks are observed slightly around 3318 cm⁻¹,

maintaining similar characteristics. For PVP K90, 1461.31 cm^{-1} (C-H bending of CH₂), and its distinctive peaks at 2594 cm^{-1} (C-H stretching), 1285.68 cm^{-1} (C-N stretching) are depicted stretching), 1649.44 cm^{-1} (C=O stretching), (Figure 3B).

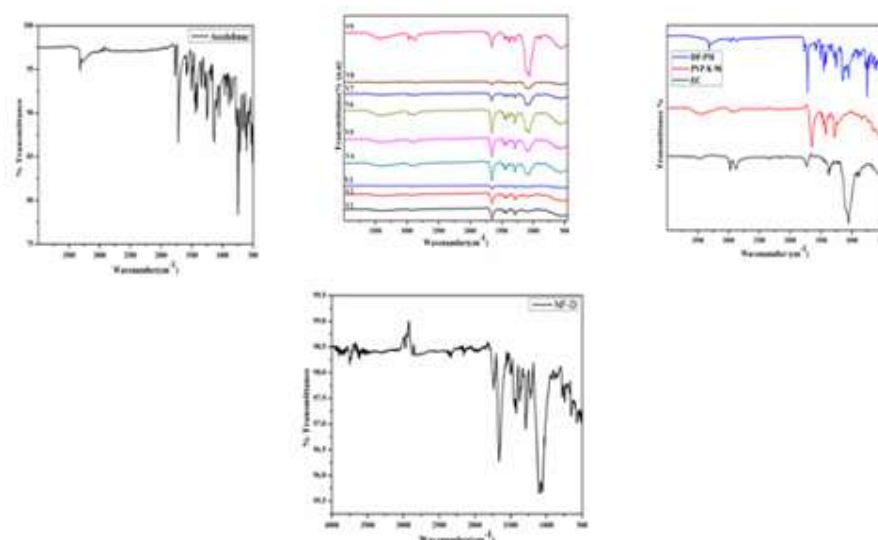


Figure No, 3 : Aceclofenac FT-IR spectra (A), Aceclofenac loaded fiber FT-IR spectra (B), Comparison of FT-IR spectra between EC, PVP K90, (C), Comparison of FT-IR spectra between V1 to V9 (D)

The distinctive absorption peaks of ethyl cellulose can be identified at 1052 cm^{-1} , attributed to C-O-C stretching, and at 2880 cm^{-1} and 2970 cm^{-1} , corresponding to C-H stretching. Additionally, a noticeable band at 3500 cm^{-1} arises from O-H stretching. As the concentration of ethyl cellulose in the fiber rises, the intensity of these peaks strengthens, while conversely, a decrease in concentration of PVP K90 results in a slight reduction in peak intensity (Figure 4D). The latter could refer to that the dissolved initially crystalline aceclofenac remained amorphous in the nanofibrous. The latter could refer to that the dissolved initially crystalline aceclofenac remained amorphous in the nanofibrous formulation (Figure 4C).

Process optimization for the fabrication of VDPF

The first step in the optimization of design parameter for fabrication of VDPF was to pick the solvent system which would act as the carrier for the polymer. For fabrication of VDPF loaded polymer solution firstly with various solvents used like water, ethanol and acetone was selected and keeping the distance between the needle and the collecting drum at 9 mm, the operational voltage at 19Kv, RPM of the collecting drum at 400-600, the flow rate of the polymer solution at 0.02ml/min. Three different polymer concentration of 10, 15 and 20% w/v of EC and PVPK90 were prepared. No fiber was formed in all the three concentration and in the case of 10 and 15 % EC and PVPK90 w/v there was only spraying. In the case of 20% EC and PVPK90 w/v since the solution was highly viscous the solution didn't escape from the needle. Details are shown in Table No.13

Table No.7: Selection of solvent system for the fabrication of VDPF.

Sr.No	Polymer Concentration % w/v	Observation
Solvent- water		
1	10%	Only spraying of the polymer solution was observed
2	15%	Only spraying of the polymer solution was observed
3	20%	Solution was too viscous it can't be push through the syringe
Solvent- DMF		
1	10%	Only spraying of the polymer solution was observed.
2	15%	Only spraying of the polymer solution was observed.
3	20%	Solution was too viscous it can't be push through the syringe
Note: Distance between the needle and the collecting drum at 9 mm, the operational voltage at 15 and 17Kv, RPM of the collecting drum at 400-600, the flow rate of the polymer solution at 0.02, 0.05 ml/min are constant.		

To overcome this problem it was decided to add a polarizing solvent in the polymer mixture to increase its ability to fabricate fibers. In this experiment, the solvent mixture selected was Ethanol. The Table No.18 lists the various combination of the variable-voltage, flow rate and polymer concentration was given. From this Table,

the optimized parameter for the fabrication of VDPF was obtained from the serial no. 39, which corresponds to 20% EC and 15% PVPK90 concentration w/v, 18.5kV and 0.5ml/min flow rate. This operating condition was used for all further experiments Table No. 14

Table No.8: Optimization of process parameters for the fabrication of VDPF

Sr.No.	Polymer conc.(w/v)		Voltage (kv)	Flow rate (ml/min)	observation
	EC	PVPK90			
1	10	10	15	0.02	Spraying was observed
2	10	10	15	0.02	Spraying was observed
3	10	10	15	0.02	Spraying was observed
4	10	10	17	0.03	Spraying was observed
5	10	10	17	0.03	Spraying was observed
6	10	10	17	0.03	Spraying was observed
7.	11	11	15	0.2	Spraying was observed
8	11	11	15	0.03	Spraying was observed
9	11	11	15	0.03	Spraying was observed
10	11	11	17	0.02	Spraying was observed
11	11	11	17	0.02	Spraying was observed
12	11	11	17	0.3	Spraying was observed
13	12	12	15	0.04	Spraying was observed
14	12	12	15	0.4	Spraying was observed
15	12	12	15	0.04	Spraying was observed
16	12	12	18	0.05	Spraying was observed
17	12	12	18	0.05	Spraying was observed
18	12	12	18	0.05	Spraying was observed
19	13	13	18	0.4	Spraying was observed



20	13	13	18	0.03	Electrospinning was observed but the result was not satisfactory.
21	13	13	18	0.05	Electrospinning was observed but the result was not satisfying as the fiber on the aluminium foil was very thin.
22	13	13	21	0.05	Fiber was obtained but the fibers were not peeling off the aluminium foil.
23	13	13	19	0.05	Fiber was obtained but the fibers were not peeling off the aluminium foil.
24	13	13	19	0.05	Fiber was obtained but the fibers were not peeling off the aluminium foil.
25	14	14	20	0.02	Fiber was obtained but the fibers were not peeling off the aluminium foil.
26	14	14	18	0.2	Fiber was obtained but the fibers were not peeling off the aluminium foil.
27	14	14	18	0.03	Fiber was obtained but the fibers were not peeling off the aluminium foil.
28	13	14	21	0.04	Fiber was obtained but the fibers were not peeling off the aluminium foil.
29	14	14	19	0.3	Fiber was obtained but the fibers were not peeling off the aluminium foil.
30	16	14	20	0.05	Fiber was obtained but the fibers were not peeling off the aluminium foil.
31	15	15	15	0.02	Spraying of fiber on to the surrounding of the collecting plate.
32	15	15	17	0.03	Spraying of fiber on to the surrounding of the collecting plate.
33	16	15	20	0.4	Spraying of fiber on to the surrounding of the collecting plate.
34	15	15	20	0.04	Spraying of fiber on to the surrounding of the collecting plate.
35	19	15	20	0.04	Spraying of fiber on to the surrounding of the collecting plate.
36	20	15	18.5	0.5	Very good fiber was obtained. This parameter was selected for all future fiber fabrication.
37	21	16	15	0.03	Spraying of fiber on to the surrounding of the collecting plate.

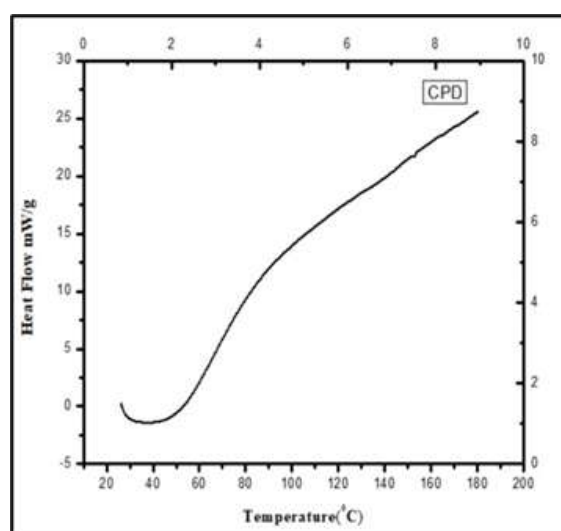
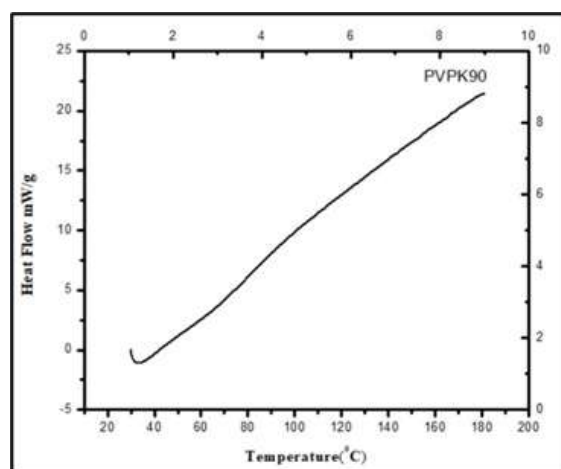
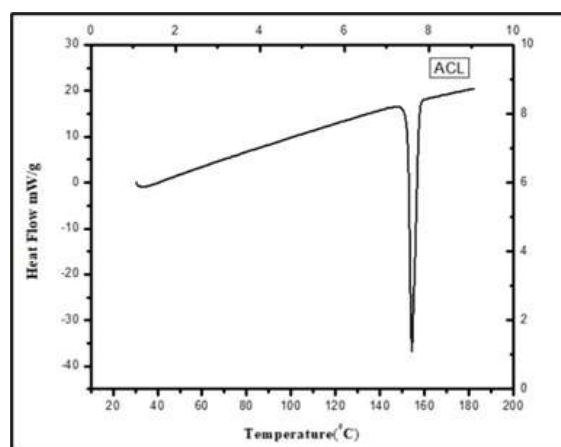
Differential scanning calorimetry (DSC)

DSC studies were performed to characterize the solid state of drugs and polymers. Further, compatibility between drug and excipients can be evaluated by observing the thermal behaviour of compounds such as appearance or disappearance of an endothermic or exothermic peak. If all the peaks remain the same, compatibility can be expected. DSC thermogram of ACL, EC, PVPK90

and optimized nanofiber membrane are depicted in Figure No.14. DSC thermogram of ACL showed a sharp endothermic peak at 155°C which is attributed to its melting point. The sharp melting peaks exhibited by ACL confirmed their existence as a crystalline form. Thermogram of EC exhibited a characteristic peak at 40°C due to its semi-crystalline nature. The PVPK90 also exhibited characteristic peaks of all components indicating physical compatibility between

excipients and drug. Whereas, optimized VDPF membrane showed flat curve without sharp endothermic or exothermic peaks of drug. This indicates that transformation of phase i.e. crystalline state to amorphous state has taken place, during the entrapment process. This might

be due to shear stress provided by the stirrer and electrospinning during the fabrication process of nanofiber which may prevent the recrystallization of ACL, leaving ACL in molecular dispersion form inside the VDPF membrane as shown in **Figure No. 5**



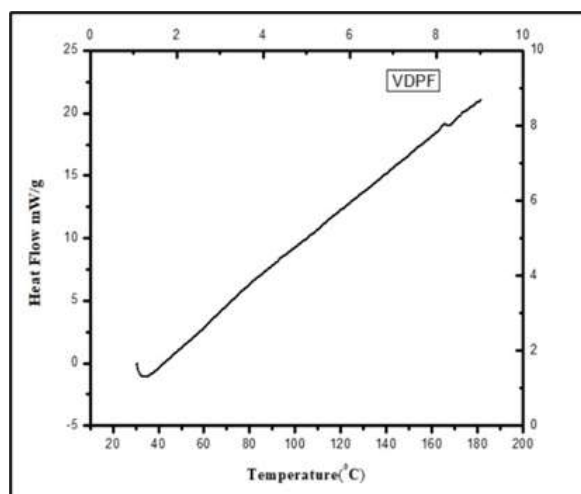


Figure No. 5 : DSC thermograms of ACL, EC, PVPK90 and optimized formulation (VDPF)

X ray diffraction studies (XRD)

To understand the crystallinity of the drug in the nanofiber membrane, XRD pattern of pure drug, CPD and their optimized VDPF membrane were recorded. The XRD pattern of ACL, as shown in **Figure No 16**. Exhibited four characteristic peaks at 2θ of 10.2° , 17.9° , 20.7° and 25° which demonstrates crystalline nature of the drug. CPD

showed two peaks in the diffractogram at a diffraction angle of 10° and 20° indicates semi-crystalline nature of CPD. Whereas, XRD pattern of VDPF membrane exhibited more of an amorphous nature as compared to pure ACL due to shifting of its diffraction intensity, conforming ACL physical state transformed from crystalline state to amorphous state during the entrapment process in the nanofiber membrane.

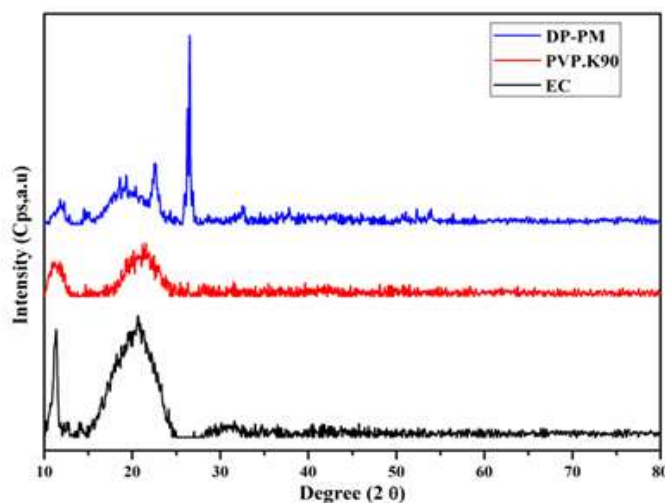


Figure No. 6 : Overlay of Powder XRD pattern of ACL, CPD and VDPF

Scanning Electron Microscopy (SEM)

The morphology of the nanofibers was examined using a scanning electron microscope (SEM). Samples were affixed to double-sided carbon adhesive tape and then coated with a sputtered

gold conductive layer using the JEOL JFC-1200 Fine Coate. SEM images were captured with a JEOL JSM-6380LA scanning electron microscope at magnifications of $500\times$, $1500\times$, and $5000\times$. Fiber diameters were measured using ImageJ software (US National Institutes of Health,

Bethesda, MD, USA), with measurements based on 50 randomly selected individual filaments at 5000× magnification. Subsequently, the average fiber diameter was calculated. SEM analysis was employed to examine the morphology of the

nanofibers obtained in the study. Figure 3 displays SEM images of samples composed of 25% PVP and 20% ethyl cellulose, with an emitter-to-collector distance of 12.5 cm.

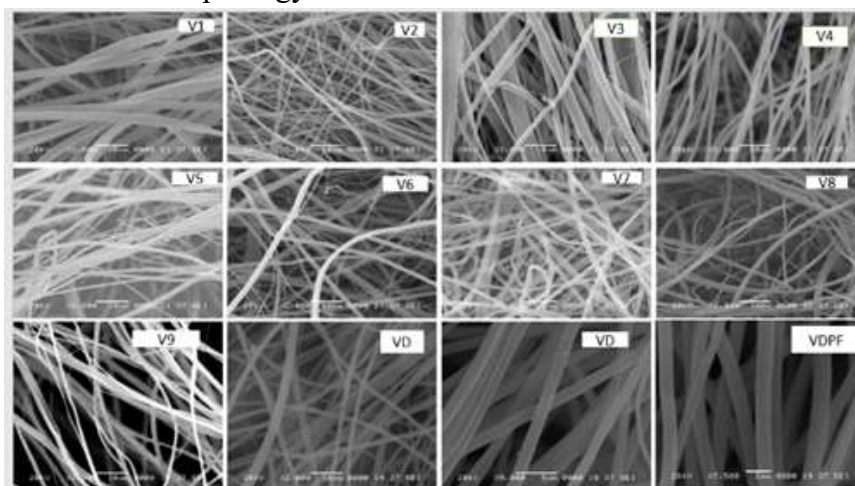


Figure No. 7: SEM Images of drug , polymer with their ratios and final optimized NF

Among all samples (V1-V9), V6 exhibited a particularly smooth and favourable property for drug loading. The formation of the film was attributed to the transition of polymeric carriers from a glassy to a rubbery state. Fibers containing 15% PVP and 20% ethyl cellulose demonstrated the most suitable characteristics for their intended application. These fibers had diameters ranging from approximately 200 to 800 nanometers, with an average diameter of 596 ± 215 nm, and displayed smooth and uniform surfaces. Consequently, composition V6 was selected for further investigations. Increasing the concentration of ethyl cellulose in the composite fibers led to a noticeable transformation in the nanofiber structure, shifting towards a smoother film formation. This alteration significantly improved the sustained release characteristics, which was observed to correlate with the polymer ratio within the composite fibers. SEM photos, as depicted in Figure 3, visually captured this phenomenon. The rationale behind this shift lies in the enhanced molecular mobility facilitated by the presence of plasticizers in the fibers. As the

concentration of ethyl cellulose increased, the plasticized fibers exhibited greater molecular mobility. Consequently, this resulted in a decrease in the inner cohesion within the polymeric chains, ultimately reshaping the structure of the fibers towards smoother film formation. This structural transformation, in turn, contributed to the enhancement of sustained release properties, making it an essential aspect in controlled-release formulations.

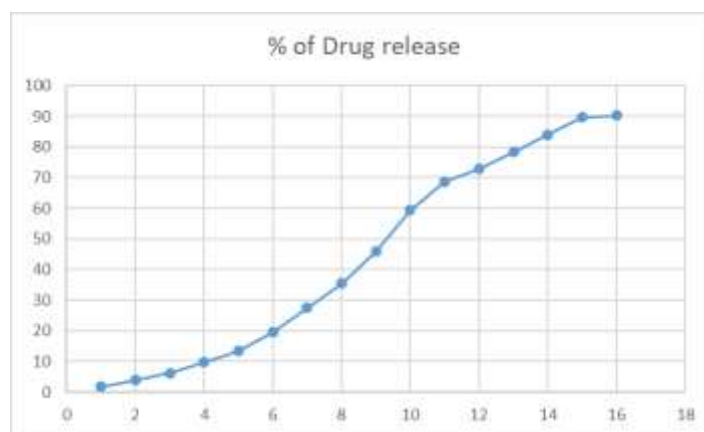
IN VITRO DRUG RELEASE STUDY

An in vitro study was conducted using a magnetic stirrer to investigate the release of a drug from a fiber. The experiment began by preparing a stock solution, where 100 mg of the drug-loaded fiber was added to 100 ml of phosphate buffer solution (1 M, pH 6.8), and stirred at 100 rpm for 16 hours. At hourly intervals, 10 ml of the solution was withdrawn from the stock, and an equal volume of fresh buffer solution was added to maintain the volume. Each withdrawn sample was then analyzed for absorbance at 277 nm using a

spectrophotometer. By analyzing the absorbance data, it was determined that approximately 90.19% of the drug had been released into the buffer solution by the end of the 16-hour period. This study provides insights into the release kinetics of the drug from the fiber in vitro, which is crucial for understanding its potential applications in drug delivery systems.

Table No.8: % of Drug release on each hour

Sr. No.	Time/ Hr	% Drug Release
1	1	1.75
2	2	3.9
3	3	6.24
4	4	9.75
5	5	13.47
6	6	19.52
7	7	27.52
8	8	35.53
9	9	45.88
10	10	59.35
11	11	68.72
12	12	72.82
13	13	78.28
14	14	83.95
15	15	89.61
16	16	90.19

**Figure No.8: The % Of Drug Release at Each Hour**

CONCLUSION:

This study demonstrated that the nanofiber formed successfully with chosen composition of polymer and drug with highest drug loading of 90 %. As expected, the nanofiber releases the drug in a sustained way for up to 16 hrs. The SEM studies confirmed the nanofibrous structure, while the FT-IR and DSC tests can indicate that the originally crystalline properties of aceclofenac in the formulations. From the results we concluded that the formulated NF acts as a promising alternative in the therapy of osteoarthritis and rheumatoid

arthritis with an enhanced rate and extent of absorption due to the improved wettability and dissolution rate thus providing smaller effective doses and causing fewer potential side effects.

REFERENCES

1. Aceclofenac. Available online: <https://www.drugbank.ca/drugs/DB06736> (accessed on 20 December 2023).
2. Lanas, A.; Chan, F.K. Peptic ulcer disease. *Lancet* 2017, 390, 613–624. [CrossRef]



3. Day, R.; Graham, G. The vascular effects of COX-2 selective inhibitors. *Aust. Prescr.* 2004, 27, 142–145. [CrossRef]
4. Kienzler, J.L.; Gold, M.; Nollevaux, F. Systemic bioavailability of topical diclofenac sodium gel 1% versus oral diclofenac sodium in Healthy Volunteers. *J. Clin. Pharmacol.* 2010, 50, 50–61. [CrossRef] [PubMed]
5. Dooley, M.; Spencer, C.M.; Dunn, C.J. Aceclofenac. A reappraisal of its use in the management of pain and rheumatic disease. *Drugs* 2001, 61, 1351–1378. [CrossRef] [PubMed]
6. Dooley, M.; Spencer, C.M.; Dunn, C.J. Aceclofenac. A reappraisal of its use in the management of pain and rheumatic disease. *Drugs* 2001, 61, 1351–1378. [CrossRef] [PubMed]
7. Diaz-Gonzalez, F.; Sanchez-Madrid, F. NSAIDs: Learning new tricks from old drugs. *Eur. J. Immunol.* 2015, 45, 679–686. [CrossRef]
8. Raza, K.; Kumar, M.; Kumar, P.; Ruchi, M.; Gajanand, S.; Manmeet, K.; Katare, O.P. Topical delivery of aceclofenac: Challenges and promises of novel drug delivery systems. *BioMed Res. Int.* 2014, 2014, 406731. [CrossRef]
9. Pareek, A.; Chandurkar, N. Comparison of gastrointestinal safety and tolerability of aceclofenac with diclofenac: A multicenter, randomized, double-blind study in patients with knee osteoarthritis. *Curr. Med. Res. Opin.* 2013, 29, 849–859. [CrossRef]
10. Chakraborty, C.; Pal, S.; Doss, G.P.; Wen, Z.H.; Lin, C.S. Nanoparticles as ‘smart’ pharmaceutical delivery. *Front. Biosci. (Landmark Ed.)* 2013, 18, 1030–1050. [CrossRef]
11. McNeil, S.E. Unique Benefits of Nanotechnology to Drug Delivery and Diagnostics. In *Characterization of Nanoparticles Intended for Drug Delivery*; McNeil, S.E., Ed.; Humana Press (Springer Science+Business Media): New York, NY, USA, 2010; pp. 3–8. [CrossRef]
12. Yu, D.-G.; Zheng, X.-L.; Yang, Y.; Li, X.-Y.; Williams, G.R.; Zhao, M. Immediate release of helicid from nanoparticles produced by modified coaxial electrospinning. *Appl. Surf. Sci.* 2019, 473, 148–155. [CrossRef]
13. Pillay, V.; Dott, C.; Choonara, Y.E.; Tyagi, C.; Tomar, L.; Kumar, P.; du Toit, L.C.; Ndesendo, V.M.K. A review of the effect of processing variables on the fabrication of electrospun nanofibers for drug delivery applications. *J. Nanomater* 2013, 2013, 789289. [CrossRef]
14. Irfan, M.; Rabel, S.; Bukhtar, Q.; Qadir, M.I.; Jabeen, F.; Khan, A. Orally disintegrating films: A modern expansion in drug delivery system. *Saudi Pharm. J.* 2016, 24, 537–546. [CrossRef]
15. Dixit, R.P.; Puthli, S.P. Oral strip technology: Overview and future potential. *J. Control. Release.* 2009, 139, 94–107. [CrossRef]
16. Karthikeyan, K.; Guhathakarta, S.; Rajaram, R.; Korrapati, P.S. Electrospun zein/eudragit nanofibers based dual drug delivery system for the simultaneous delivery of aceclofenac and pantoprazole. *Int. J. Pharm.* 2012, 438, 117–122. [CrossRef]

HOW TO CITE: Dr. Omprakash Bhusnure, Vedant Mane, Shivam Vyavahare, Dr. Mani Ganesh, S. G. Zingade, Dr. Vijayendra Swammy, Dr. Hyun Tae Jang, Engineered Nanofiber Based Carrier to Manage Arthritis and Inflammation, *Int. J. of Pharm. Sci.*, 2025, Vol 3, Issue 6, 5504-5516. <https://doi.org/10.5281/zenodo.15762721>

